Excitation of bound plasmons along nanoscale stripe waveguides: a comparison of end and grating coupling techniques

C. S. Perera,[1,2,*] K. C. Vernon,[1,2] A. M. Funston,[3] H. Cheng,[4] F. Eftekhari,[5] and T. J. Davis[5,6]

[1]*Plasmonic Device Group, Queensland University of Technology, Brisbane 4001, QLD, Australia*
[2]*Institute for Future Environments, Queensland University of Technology, Brisbane 4001, QLD, Australia*
[3]*School of Chemistry, Monash University, Clayton 3800, VIC, Australia*
[4]*Australian National Fabrication Facility QLD Node, AIBN, University of Queensland, St. Lucia 4072, QLD, Australia*
[5]*Melbourne Centre for Nanofabrication, Clayton 3169, VIC, Australia*
[6]*CSIRO Manufacturing Flagship, Clayton 3169, VIC, Australia*
[*]*cp.hettiarachchige@qut.edu.au*

Abstract: In this paper we excite bound long range stripe plasmon modes with a highly focused laser beam. We demonstrate highly confined plasmons propagating along a 50 μm long silver stripe 750 nm wide and 30 nm thick. Two excitation techniques were studied: focusing the laser spot onto the waveguide end and focusing the laser spot onto a silver grating. By comparing the intensity of the out-coupling photons at the end of the stripe for both grating and end excitation we are able to show that gratings provide an increase of a factor of two in the output intensity and thus out-coupling of plasmons excited by this technique are easier to detect. Authors expect that the outcome of this paper will prove beneficial for the development of passive nano-optical devices based on stripe waveguides, by providing insight into the different excitation techniques available and the advantages of each technique.

OCIS codes: (050.2770) Gratings;(240.0240) Optics at surfaces;(240.6680) Surface plasmons.

References and links

1. S. Lal, S. Link, and N. J. Halas, "Nano-optics from sensing to waveguiding," Nat. Photonics **1**(11), 641–648 (2007).
2. H. A. Atwater and A. Polman, "Plasmonics for improved photovoltaic devices," Nat. Mater. **9**(3), 205–213 (2010).
3. R. Charbonneau, C. Scales, I. Breukelaar, S. Fafard, N. Lahoud, G. Mattiussi, and P. Berini, "Passive integrated optics elements based on long-range surface plasmon polaritons," J. Lightwave Technol. **24**(1), 477–494 (2006).
4. P. Berini, "Long-range surface plasmon polaritons," Adv. Opt. Photonics **1**(3), 484–588 (2009).
5. A. Boltasseva, T. Nikolajsen, K. Leosson, K. Kjaer, M. S. Larsen, and S. I. Bozhevolnyi, "Integrated optical components utilizing long-range surface plasmon polaritons," J. Lightwave Technol. **23**(1), 413–422 (2005).
6. I. Breukelaar, P. Berini, and P. Berini, "Long-range surface plasmon polariton mode cutoff and radiation in slab waveguides," J. Opt. Soc. Am. A **23**(8), 1971–1977 (2006).
7. G. Bracher, K. Schraml, C. Jakubeit, M. Kaniber, and J. Finley, "Direct measurement of plasmon propagation lengths on lithographically defined metallic waveguides on GaAs," J. Appl. Phys. **110**(12), 123106 (2011).
8. I. Salakhutdinov, J. S. Thakur, and K. Leosson, "Characterization of long-range surface plasmon-polariton in stripe waveguides using scanning near-field optical microscopy," J. Appl. Phys. **102**(12), 123110 (2007).
9. H. Ditlbacher, J. R. Krenn, G. Schider, A. Leitner, and F. R. Aussenegg, "Two-dimensional optics with surface plasmon polaritons," Appl. Phys. Lett. **81**(10), 1762–1764 (2002).
10. K. Vernon, D. Gómez, and T. Davis, "A compact interferometric sensor design using three waveguide coupling," J. Appl. Phys. **106**(10), 104306 (2009).
11. P. Berini, "Plasmon-polariton waves guided by thin lossy metal films of finite width: Bound modes of asymmetric structures," Phys. Rev. B **63**(12), 125417 (2001).
12. B. Wang and G. P. Wang, "Simulations of nanoscale interferometer and array focusing by metal heterowaveguides," Opt. Express **13**(26), 10558–10563 (2005).

13. R. Buckley and P. Berini, "Figures of merit for 2D surface plasmon waveguides and application to metal stripes," Opt. Express **15**(19), 12174–12182 (2007).
14. J. Krenn, B. Lamprecht, H. Ditlbacher, G. Schider, M. Salerno, A. Leitner, and F. Aussenegg, "Non–diffraction-limited light transport by gold nanowires," Europhys. Lett. **60**(5), 663–669 (2002).
15. B. Lamprecht, J. R. Krenn, G. Schider, H. Ditlbacher, M. Salerno, N. Felidj, A. Leitner, F. R. Aussenegg, and J. C. Weeber, "Surface plasmon propagation in microscale metal stripes," Appl. Phys. Lett. **79**(1), 51–53 (2001).
16. R. Zia, M. D. Selker, and M. L. Brongersma, "Leaky and bound modes of surface plasmon waveguides," Phys. Rev. B **71**(16), 165431 (2005).
17. C. Chen and P. Berini, "Grating couplers for broadside input and output coupling of long-range surface plasmons," Opt. Express **18**(8), 8006–8018 (2010).
18. E. D. Palik, *Handbook of Optical Constants of Solids* (Elsevier Science and Tech, 1985).
19. G. Ghosh, "Dispersion-equation coefficients for the refractive index and birefringence of calcite and quartz crystals," Opt. Commun. **163**(1-3), 95–102 (1999).
20. A. Giannattasio, I. R. Hooper, and W. L. Barnes, "Dependence on surface profile in grating-assisted coupling of light to surface plasmon-polaritons," Opt. Commun. **261**(2), 291–295 (2006).
21. S. A. Maier, *Plasmonics: Fundamentals and Applications* (Springer, 2007).

1. Introduction

The use of plasmon waveguides for the development of sensitive nanoscale sensors and passive optical devices is a hot topic in photonics research [1–3]. A common plasmon waveguide design is the metal slab waveguide, which supports two surface plasmon polariton (SPP) modes on the upper and lower interface. These modes can couple together, forming symmetric and asymmetric modes depending on the orientation of the main E-field component [4, 5]. The symmetric mode attenuation dramatically decreases with reducing metal thickness resulting in Long Range Surface Plasmon Polaritons (LRSPPs). A metal slab with different upper and lower dielectric media can also support LRSPPs but has a mode cut-off thickness, below which the LRSPP is no longer bound and guided [4, 6].

Metal stripe waveguides are based on metal slab waveguides but have a finite width. They are one of the simplest waveguide structures that allow nanoscale confinement of the light in two dimensions. Commonly, they consist of a metallic rectangular bar surrounded by a dielectric medium, and theoretically can also support LRSPPs which propagate micron distances at or near visible excitation. Many stripe waveguide experiments are carried out in the IR or near IR ranges and these have proven the existence of the LRSPP [5, 7–9]. Whilst a number of theoretical papers based on stripe waveguide excitation in the visible predict the existence of bound LRSPP plasmon modes, there has been no experimental confirmation of this [10–13]. Several experiments have been reported in the visible for the detection of leaky plasmon modes supported by stripe waveguides [11, 14–16]. These waveguides often sit on a substrate and are exposed to air. The plasmon mode supported by the waveguide leaks into the air region and its presence is detected via near field scanning optical microscopy techniques [14]. However such waveguides do not provide the same level of field confinement in two dimensions due to the leaky nature of their modes.

Stripe waveguides are popular as a plasmon waveguide due to the long propagation lengths achieved and the simplicity of the geometry compared to other waveguides [3, 13]. However, nanoscale confinement and guided propagation of bound plasmons by these waveguides has been difficult to achieve in the visible. In this paper we investigate bound plasmon modes supported by stripe waveguides under visible excitation. Two excitation techniques are discussed – excitation of the waveguide end and excitation of a grating at the waveguide input. We define end excitation as exciting the end of a stripe waveguide by focusing a laser beam onto the stripe edge through a high NA objective. For the grating coupling, gratings were fabricated in front of the stripe waveguide and the laser beam focused through the high NA objective onto the middle of the grating. The position of the focused beam onto the grating was optimised for maximal output intensity at the stripe end.

This type of end coupling has been reported before for near IR excitation, and is also known as broadside excitation [7]. Grating excitation for stripe waveguides has not been

reported before but has been studied theoretically by Berini et al for metal slabs [17]. Authors believe this work is the first attempt to excite bound LRSPP in the visible region.

2. Theory

Silver LRSPP waveguides were designed for 640 nm excitation. The waveguides were supported by an ITO-coated glass substrate and modelled with a covering layer of SiO_2. See Fig. 1(a) for a schematic of the waveguide design.

The width of the Ag waveguides was chosen as 750 nm, and the thickness of the waveguide was varied so that only one long range mode was supported. Using COMSOL Multiphysics the modes supported by the waveguide for various waveguide thickness was calculated, along with the propagation lengths. The permittivity of silver was taken as −16.4 + 1.13i [18], ITO as 3.42 + 0.22i from Sopra database, glass 2.3 and SiO_2 as 2.4 [19]. The thickness of the ITO was set to 15 nm. The wavenumber of the long range guided modeand propagation length are shown in Fig. 2. Plasmon propagation length (L_p) is taken as the distance the plasmon travels before its intensity drops by a factor of e.

As can be seen from Fig. 2(a), the long range guided mode's wavenumber increases with increasing thickness of the metal film. This indicates that the mode becomes more localised as the metal film thickness increases, resulting in more of the plasmon being confined inside the metal. This localisation results in a decrease in the propagation distance of the mode as the film thickness increases, due to the inherent losses of the metal, Fig. 2(b). Such behaviour is typical of long range modes in asymmetric stripe structures, of low asymmetry [6]. As the metal film thickness increases the mode becomes more localised to one of the stripe edges resulting in higher confinement (larger wavenumber) and thus smaller propagation length.

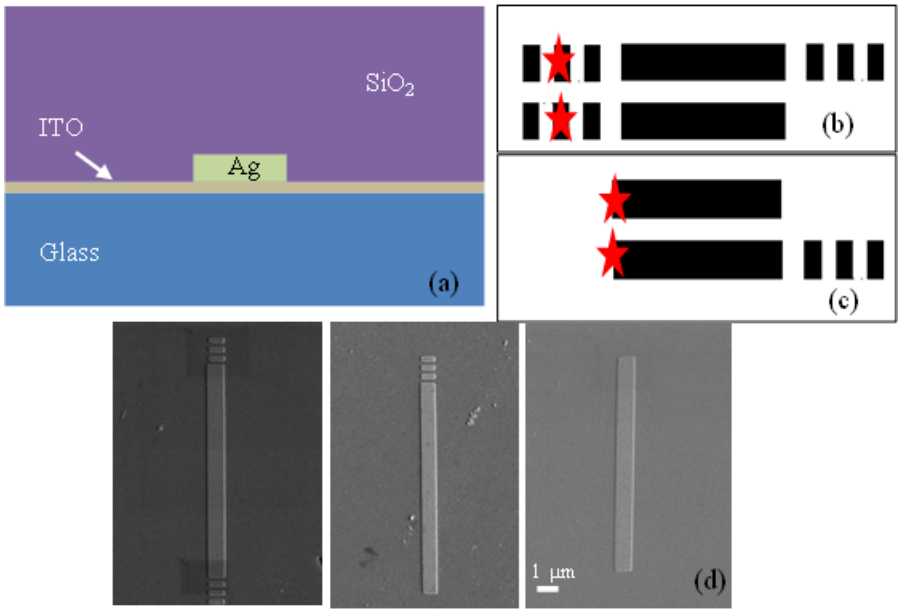

Fig. 1. Schematic of the coupling arrangements of the structures (not to scale): (a) Front-on schematic of sample (b) grating coupling (c) end coupling. Here star represents the laser spot. (d) SEM images of the three structures (width 750 nm, length 10 μm and thickness 30 nm).

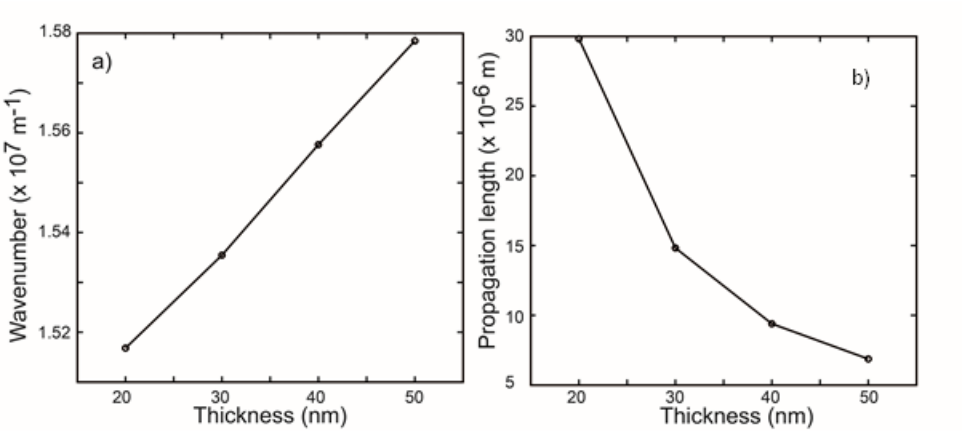

Fig. 2. (a) Wavenumber, (b) Propagation length of the LRSPP mode and their dependence on thickness.

It was found that if the stripe thickness was decreased below 20 nm, the long range mode would be cut-off and no longer bound. Also, if the thickness was above 40 nm, two long range modes existed. To ensure only one long range mode, a thickness of 30 nm was selected. For this thickness, the plasmon has a 15 micron propagation distance. The field profile of this long range plasmon mode is shown in Fig. 3.

In this paper, we test different excitation methods for exciting the LRSPP mode. Several waveguide geometries were fabricated, one without gratings, one with an input grating, one with an output grating, and one with input and output gratings. The schematic of the various ready-to excite waveguides are shown in Figs. 1(b) and 1(c).

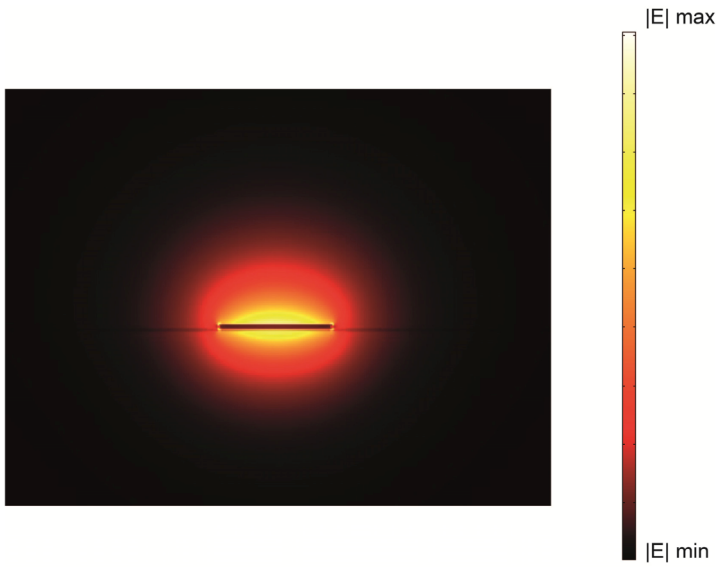

Fig. 3. |E| field plot of the LRSPP mode in a 30 nm thick, 750 nm wide waveguide on ITO coated glass.

The grating periodicity and height were selected to achieve high efficiency and to preferentially excite the LRSPP mode. Grating causes the incident LRSPP to be partially reflected in opposite direction to plasmon propagating direction. This perturbation can be reduced by strengthening the grating structure such that partial reflections of adjacent bumps

cancel out [17]. It has been proven theoretically, and experimentally in the case of square gratings, that light-SPP coupling is maximised when the groove-to-pitch ratio is equal to ½ for SPs supported by metal films [20]. Since the long range mode of the stripe waveguide has a similar field profile to the SP [17] we use the same grating formula to calculate the grating period and a groove-to-pitch ratio of ½. Using the grating equation, the wavenumber of the plasmon (β) excited by the grating is [21]

$$\beta = k\sin\theta + \frac{2\pi m}{a} \tag{1}$$

where k is the incident beam wavenumber, θ is its angle of incidence, a is the grating periodicity and m is the grating order. In our experiment the laser beam was focused at near-normal incidence on the substrate using high numerical aperture objective. Thus Eq. (1) can be approximated as

$$\beta = \frac{2\pi m}{a} \tag{2}$$

And for the 1st grating order this gives

$$\beta = \frac{2\pi}{a} \tag{3}$$

The grating period for our system is 416 nm.

There are some disadvantages with grating excitation, as discussed by Berini et al in the case of metal slabs [17]. Grating excitation not only produces the desired LRSPP mode but also other radiation modes which can affect the power of the out-coupled light from the waveguide. The total power propagating along the waveguide ($-x$ direction) at x can be written as [17]

$$P_x(x) = P_{S0}e^{2\alpha(x-x_0)} + P_{rad}(x) \tag{4}$$

where P_{S0} is the power carried by the LRSPP at $x = x_0$ (x_0 is the location of the left edge of the grating), α is the field attenuation constant of the LRSPP and $P_{rad}(x)$ is the power carried by all the other modes. Similar issues can be encountered with end excitation. The stripe edge basically operates as a surface defect [21] allowing the generation of multiple plasmon modes when the highly focused laser beam strikes the waveguide edge. However, all other modes supported by these carefully designed stripe waveguides have very low propagation lengths (< 2 μm).Both end and grating excitation techniques will be studied in this paper.

3. Method

3.1 Fabrication

Plasmonic waveguides were patterned on a 300 nm bilayer PMMA resist(950k A4 / 495 k A4 PMMA resist from Microchem GmbH) using electron beam lithography (JEOL-7800 FE-SEM with Raith Quantum Elphy) with a beam current of ~75 pA and 20 kV acceleration voltage under optimal dose of 280 μC/ cm^2. Patterned PMMA layer was then developed for 30 seconds in MIBK:IPA 1:3 solution. 30 nm Ag was evaporated on the developed sample using the PVD 75 e-beam evaporator under a slow rate of 0.27 °A/s. Scanning electron microscope image shows the 750 nm wide stripes survived successfully after lift- off in acetone bath. A 200 nm SiO_2 layer was then evaporated (with a rate of 0.5°A/s) on top of the waveguides to ensure waveguiding in the desired mode. We fabricated stripes with gratings on both ends, grating one end and no grating for different stripe lengths (5 μm, 10 μm, 20 μm,

30 µm, 40 µm, 50 µm) Refer Fig. 1(b). SEM image of three waveguides (one with grating at both ends, one with grating at one end and one with no grating) with 10 µm width are shown in Fig. 1(c). The grating periodicity was 416 nm with a groove to pitch ratio of ½.

3.2 Experimental setup

For optical characterisation and excitation of the fabricated waveguides we used an inverted microscope. Light from a linearly polarised 640 nm diode laser was focused onto the sample via a 100x oil immersion objective with NA = 1.4. Polarisation of the excitation light was varied using λ/2 plate. Plasmon out-coupling into free space photons at the distal tip of the waveguide was observed using a CCD camera (Fig. 4). To verify the plasmon nature of the guided mode, polarisation dependence of the out-coupling light was studied.

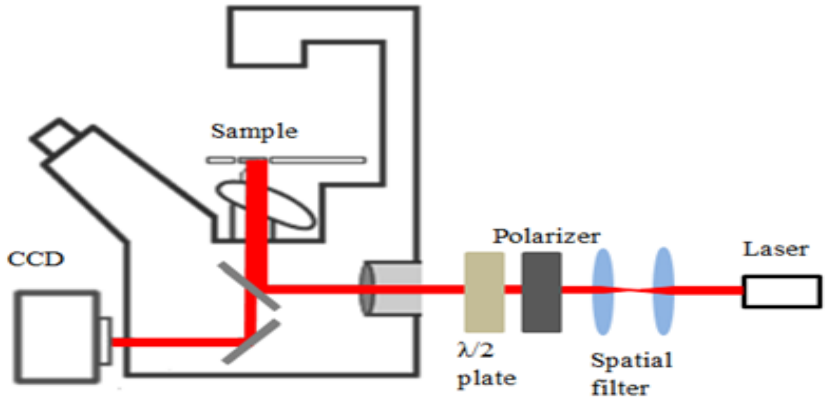

Fig. 4. Schematic diagram of the experimental set up. Objective with N/A 1.4.

4. Optical characterisation

4.1 Polarisation dependence

Figure 5 shows the experimentally measured polarisation dependency of the light out-coupled from a 20 µm long stripe excited via Fig. 5(a) and 5(b) grating excitation and Fig. 5(c) and 5(d) end excitation. The polar plots show that out-coupling is maximized when the electric field of the exciting photons are TM polarised. Calculated Degrees of Polarisation (DoP) for out-coupling intensities for plots in Fig. 5(a)-5(d) are 78%, 80%, 86% and 88% respectively.

DoP is defined as [7]

$$DoP = \frac{I_{max} - I_{min}}{I_{max} + I_{min}} \tag{5}$$

where I_{max} and I_{min} are maximum and minimum intensities of the output light at the end of the stripe waveguide.

DoP analysis shows that outcoupling light from end excitation (86-88%) is significantly TM in nature, and supports the presence of a plasmon mode [7].The end excitation DoP is also more polarised than that of grating coupling (78-80%), which is in line with the theoretical research that has shown that gratings also produced radiation modes which are not TM polarised [17].

Figure 5(d) shows CCD images of out-coupling photons from the waveguide end for 20 µm stripes with Figs. 5(d)(i) grating both sides, 5(d)(ii) excitation grating only, 5(d)(iii) no grating and 5(d)(iv) grating in the output only. It is obvious that out-coupling intensity drops when there is no grating involved in the excitation of the LRSPP.

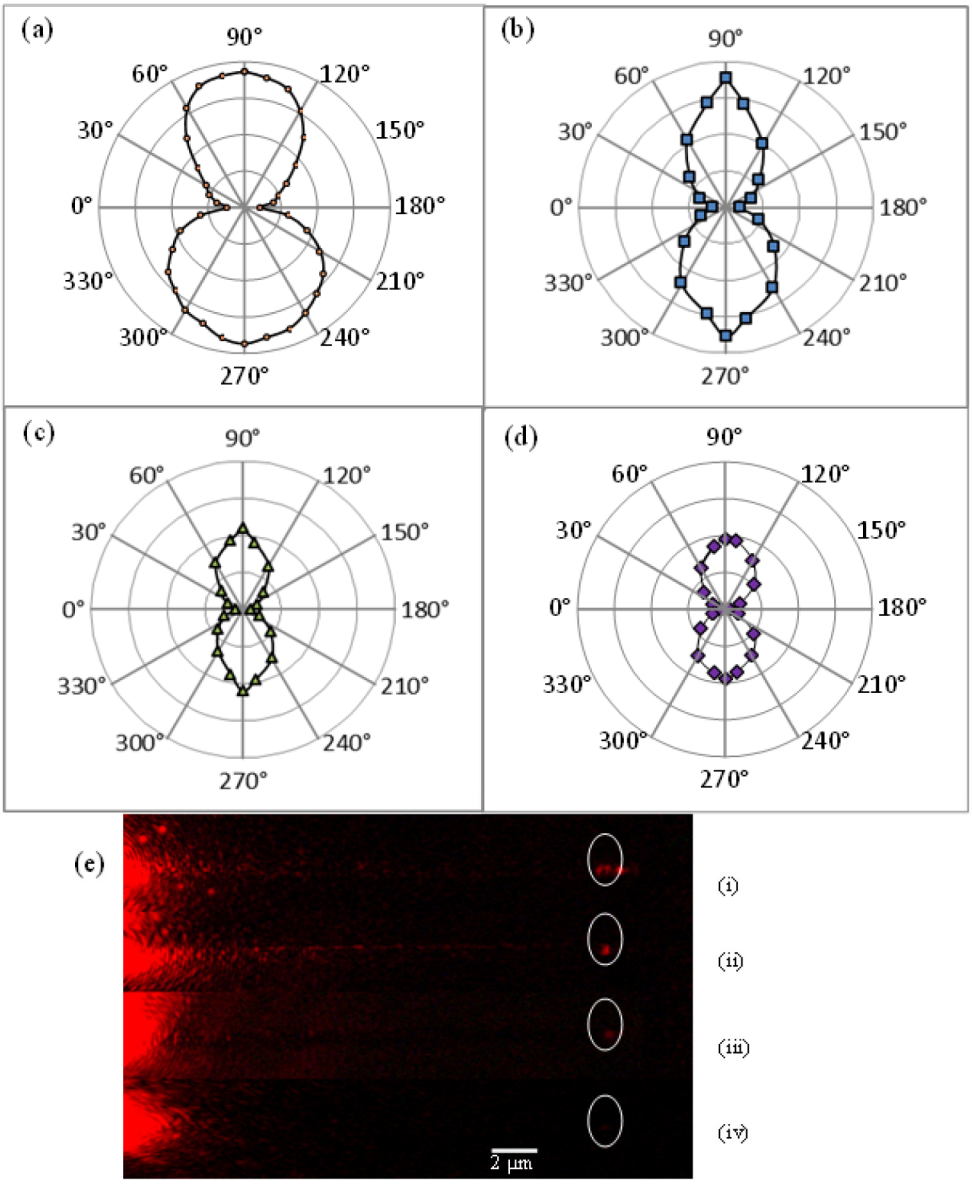

Fig. 5. Polar plots of out-coupling from (a) grating coupled stripe with grating on both side, (b) grating coupled stripe with grating on one end and (c) end coupled stripe without grating (d)end coupled stripe with grating on one end. Radial scale goes from 0 to 70 with 17.5 increments. (e) Series of CCD images of light scattering from the waveguide end 20 µm long stripe (i) grating coupled stripe with grating (ii) grating coupled stripe with grating one side (iii)end coupled stripe without grating (iv) end coupled stripe with one grating.

4.2 Propagation length

4.2.1 End coupling

To further verify that the stripes support a plasmon guided mode, the propagation length of the guided mode was investigated. Figure 6(a) shows the CCD images of the out-coupling intensity of end-coupled stripes for stripes lengths of 5 µm, 10 µm, 20 µm, 30 µm, 40 µm, while, Fig. 6(b) shows the out-coupling intensity dependence on stripe length for end

excitation. The two curves show how the presence of an out-coupling grating affects the out-coupled intensity. It is clear that the presence of an out-coupling grating does not significantly impact the output intensity.

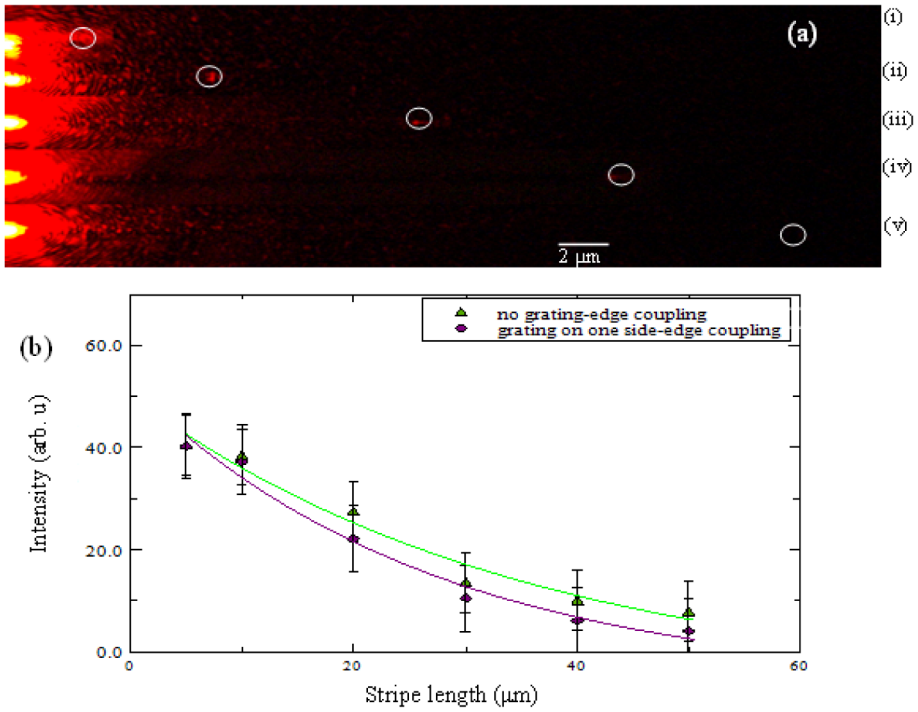

Fig. 6. (a) Series of images obtained using CCD camera. Stripes with no grating for lengths of (i)5 μm, (ii) 10 μm, (iii) 20 μm, (iv) 30 μm and (v) 40 μm. (b) Out-coupling intensity vs stripe length with exponential fit for end coupled stripes.

The out-coupling intensity for each stripe plotted in Fig. 6(b) can be used to determine the propagation length of the guided mode.

We define the propagation length L_p, as the length the plasmon travels before its initial intensity (I_0) drops by a value of e

$$L_p = \frac{I_0}{e} \tag{6}$$

By fitting an exponential to the curves in Fig. 6(b), the initial intensity I_0 is extrapolated, and the propagation length L_p determined. The propagation length is 18 ± 6 μm for stripes with gratings at in the detection channel and 20 ± 6 μm for stripe without grating which compares well with the theoretical predictions of 15 microns.

4.2.2 Grating excitation

A similar analysis has been conducted for plasmons excited via grating excitation. Figure 7(a) shows the CCD images of the out-coupling intensity of grating coupled stripes with grating both ends for stripes lengths of 5 μm, 10 μm, 20 μm, 30 μm, 40 μm, 50 μm. Figure 7(b) shows the averaged out-coupling intensity drop with the increase of stripe length for stripes excited by grating coupling. The two curves show how the presence of an output grating affects the out-coupling intensity, and once again the output grating does not have a significant affect.

However, upon comparison of Fig. 6(b) and Fig. 7(b), the intensity obtained via grating excitation is approximately double that obtained via end excitation.

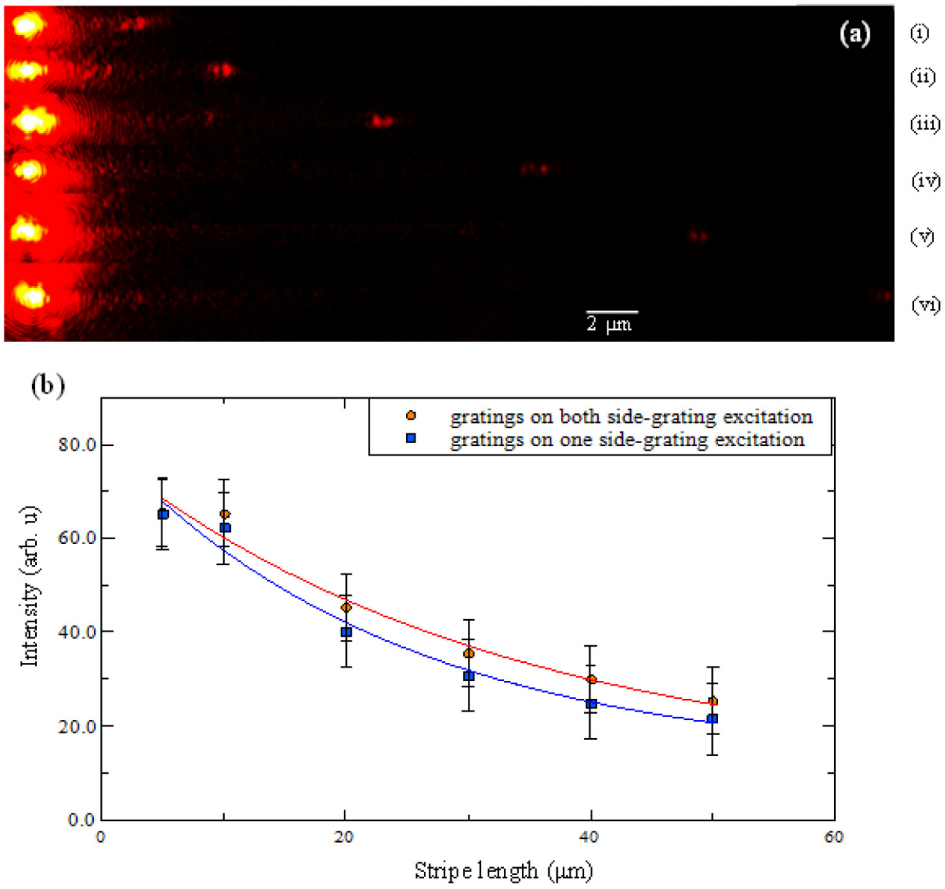

Fig. 7. (a) Series of images obtained using CCD camera. Stripes with grating either side for lengths of (i) 5 μm, (ii) 10 μm, (iii) - (vi) 50 μm with 10 μm step increment. (b) Out-coupling intensity vs stripe length with exponential fit for grating coupled stripes.

Propagation length for stripes with grating one end is 41 ± 8 μm and for stripe with grating both ends is 53 ± 7 μm. These propagation lengths are approximately two to three times that of the theoretical value of 15 μm. This discrepancy can be due to slight variation of refractive indices and thicknesses of the materials used in fabrication, but since this wasn't an issue for the end excitation, this variation in propagation length is most likely due to strong spatial transients caused by the strong involvement of radiation modes [17].

The use of grating in excitation of LRSPP on a stripe waveguide has clearly doubled the out-coupling intensity thus making the LRSPP waveguiding easier to detect visually. However, it is clear that grating excitation has resulted in the presence of other modes. From Eq. (4) it can be deduced that the effects of these radiation modes will decrease for LRSPPs that have longer propagation lengths. Thus it would seem that grating excitation would prove useful for stripes fabricated in the telecom regime where propagation lengths are much larger [17].

The grating excitation has provided almost double the output intensity at the distal end compared to that observed for end excitation. Berini et al reports the efficiency of grating coupling to be around 20% for stripe waveguides, finding that the grating excitation efficiency is higher than the efficiencies of other out-of-plane in coupling techniques to date

[17]. Thus, our findings of greater output intensity at the distal end for grating excitation vs end excitation are consistent with Berini's results. Grating excitation is designed to not only help direct light towards the waveguide but to generate only the desired plasmon mode. End coupling is similar to exciting plasmons using surface defects. It will scatter light in all directions and generate all possible modes in the stripe waveguide [21]. Since our stripe is multimodal and supports 4 bound stripe modes, it is expected that the edge excitation efficiency for our desired mode will be less than that of the grating.

In summary, we have reported optical characterization of bound LRSPPs in the visible regime. Despite their propagation length of 15 microns, we have shown that experimentally it is possible to visually detect the plasmon propagating up to 50 μm. Due to the bound nature of these LRSPPs, these plasmons have higher localisation in two dimensions than their leaky counterparts [11, 16].

We have also demonstrated that bound LRSPPs can be excited via both gratings and end excitation techniques. Polar plots depict that out-coupling LRSPP can be detected when the waveguide is excited with TM polarised photons, confirming the plasmonic nature of these modes. The grating excitation technique provides higher output intensities and easier detection than the end excitation, however, the presence of radiation modes in the grating excitation results in a lower DoP.

The advantage of end excitation is that the presence of other modes is minimal as can be seen from the DoP and the propagation length analysis. If it is important to produce single mode waveguides, end excitation is a superior technique to grating excitation. We alsodemonstrated, for end excitation, that it is possible to easily detect plasmon propagation visually up to 20 μm in the visible range.

Authors expect these findings will be beneficial for future LRSPP applications, enabling the informed decision about the best excitation technique for the particular stripe set-up.

Acknowledgments

This work was performed in parts at the Queensland node of the Australian National Fabrication Facility (ANFF), a company established under the National Collaborative Research Infrastructure Strategy to provide nano and micro-fabrication facilities for Australia's researchers and Melbourne Centre for nanofabrication (MCN) in the Victorian Node of the ANFF. CP acknowledges valuable support from the UQ AIBN, UQ CMM, and QUT CARF team. CP and KV acknowledge the Australian Research Council (ARC) grant DP110101454 and the Asian Office of Aerospace Research and Development grant FA2386-14-1-4056. AMF acknowledges the Australian Research Council (ARC) fellowship FT110100545.